

RESEARCH ARTICLE

10.1029/2018JG004924

Key Points:

- The correlation between integrated PP and Chla was not significant, and their seasonal variations differed between water masses
- C:Chla and POC:Chla were significantly higher during summer in the off-shelf waters
- A few stations in the Changjiang River plume were characterized by low NA but high PP

Correspondence to:

B. Huang,
bqhuang@xmu.edu.cn

Citation:

Liu, X., Laws, E. A., Xie, Y., Wang, L., Lin, L., & Huang, B. (2019). Uncoupling of seasonal variations between phytoplankton chlorophyll *a* and production in the East China Sea. *Journal of Geophysical Research: Biogeosciences*, 124, <https://doi.org/10.1029/2018JG004924>

Received 14 NOV 2018

Accepted 8 JUL 2019

Accepted article online 18 JUL 2019

Author Contributions:

Conceptualization: Xin Liu**Data curation:** Xin Liu, Yuyuan Xie**Funding acquisition:** Bangqin Huang**Investigation:** Xin Liu, Yuyuan Xie, Lei Wang, Lizhen Lin**Methodology:** Xin Liu, Edward A. Laws**Project administration:** Bangqin Huang**Resources:** Xin Liu, Lei Wang**Supervision:** Xin Liu, Bangqin Huang**Validation:** Edward A. Laws**Visualization:** Bangqin Huang**Writing - original draft:** Xin Liu, Yuyuan Xie**Writing - review & editing:** Xin Liu, Edward A. Laws, Yuyuan Xie, Lei Wang, Bangqin Huang

Uncoupling of Seasonal Variations Between Phytoplankton Chlorophyll *a* and Production in the East China Sea

Xin Liu^{1,2} , Edward A. Laws³ , Yuyuan Xie^{1,2} , Lei Wang^{1,2}, Lizhen Lin^{1,2}, and Bangqin Huang^{1,2}

¹State Key Laboratory of Marine Environmental Science, Xiamen University, Xiamen, China, ²Fujian Provincial Key Laboratory of Coastal Ecology and Environmental Studies, Xiamen University, Xiamen, China, ³Department of Environmental Sciences, School of the Coast and Environment, Louisiana State University, Baton Rouge, LA, USA

Abstract Phytoplankton chlorophyll *a* (Chla), primary production (PP), and nutrient uptake rates are fundamental and important parameters in marine biogeochemical studies. However, the relationships between them are associated with much uncertainty that reflects gaps in basic understanding of ecosystem dynamic. In this study, we simultaneously measured PP and nitrate assimilation (NA) along with estimated concentrations of nutrients, particulate organic carbon concentrations, phytoplankton Chla, pigments, and carbon biomass in the dynamic shelf ecosystems of the East China Sea (ECS) on four cruises during different seasons. There were large spatial gradients of these parameters, and seasonal patterns of phytoplankton Chla and PP varied between water masses. The results of this study and previous work indicated that seasonal variations of Chla and PP were similar in coastal waters but opposite in off-shelf waters. During summer in off-shelf waters, there were patches of high PP and NA associated with low Chla concentrations; this pattern was reversed in the winter. We suggest that there is a global tendency for PP and Chla patterns to be out of phase. This asynchrony is reflected mainly in the seasonal variations of C:Chla ratios driven by the combined influences of light, temperature, and nutrients. Stronger grazing pressure by microzooplankton in summer likely contributed to the high production but low biomass in the ECS. The significant correlation between PP and NA suggested that variations of PP in the ECS were driven largely by nitrate uptake, which may be inhibited by high ammonium concentrations in the Changjiang River plume.

1. Introduction

Photosynthesis accounts for most primary production (PP) in marine ecosystems and starts the flows of energy and organic matter that sustain marine fish production (Field et al., 1998). Chlorophyll *a* (Chla) is a photosynthetic pigment found in all phytoplankton and is an essential component of the photosynthetic units of all eukaryotic algae and cyanobacteria. Its concentration can be conveniently measured by a variety of techniques, including in situ probes and remote sensing of ocean color via satellites. It is thus frequently used as a metric of phytoplankton biomass (standing stock) and as a variable in equations used to estimate PP on regional and global ocean scales (Behrenfeld & Falkowski, 1997; Platt & Sathyendranath, 1988).

Areal phytoplankton carbon biomass, PP, and Chla concentrations are usually correlated, especially at large time and space scales. However, Chla is not simply a measure of phytoplankton biomass but also registers changes in intracellular pigmentation arising from light-driven (photoacclimation) and nutrient-driven physiological responses, which are not necessarily indicative of proportional changes in productivity (Behrenfeld et al., 2016). Thus, there is not always a clear relationship between Chla concentrations and PP (Laws et al., 2016). In addition, the accuracy of satellite-based, productivity-carbon flux models relies entirely on the functional relationship between Chla and PP, which is confounded by the fact that photosynthetic rates are related to factors in addition to Chla and surface irradiance (e.g., temperature, macronutrients, trace metals, and vitamins; Platt & Sathyendranath, 1988; Laws et al., 2016). Therefore, reasons for the uncoupling of variations between Chla and PP are associated with much uncertainty that reflects gaps in basic understanding of ecosystem dynamics.

To better understand the relationships between phytoplankton Chla and PP, it would be desirable to improve estimates of the phytoplankton C-to-Chla ratio (C:Chla, weight:weight), called the F-ratio by Strickland (1960). The F-ratio has been derived from data sets using empirical relationships

(Sathyendranath et al., 2009) and has been used to enable carbon-based food web calculations and carbon-based ecosystem models, which have often been validated using chlorophyll measurements (Li et al., 2010). During the 58 years since the publication of Strickland's (1960) paper, numerous studies have revealed that the C:Chla ratios of pure cultures can vary by almost 2 orders of magnitude (from single digits to several hundred g:g) as a function of species and growth conditions (Harrison et al., 1990; Hunter & Laws, 1981; Thompson et al., 2004). Assembling a large number of C biomass estimates in a natural community is difficult. The generally accepted method of estimating C biomass is based on microscope counts and volume measurements of relevant species (Harrison et al., 2015). There are extensive data sets of these parameters in well-studied regions (e.g., time series stations in the English Channel, California upwelling system, and Hawaii and Bermuda time series), and relatively clear relationships with environmental factors have emerged from laboratory studies. However, it is problematic to extrapolate laboratory or field results to other circumstances because of differences in biological communities and environmental conditions, as well as the complexity of interactions between environmental factors and biological processes in natural systems (Laws et al., 2016). Even if the community structure is stable, the effects of light (Geider et al., 1996) and nutrient (Geider et al., 1997) availability on C:Chla ratios are significant. Hence, there is still great uncertainty in the quantitative relationship between carbon biomass and Chla concentration in natural environments.

Phytoplankton standing stock, whether quantified in terms of Chla or C biomass, reflects a balance between phytoplankton production, losses due to grazing and sinking, and changes caused by advection and mixing. On a global scale, microzooplankton grazing consumes on average 60–80% of daily PP in the ocean (Calbet & Landry, 2004). Long-term results from the Baltic Sea transition zone have clearly shown that grazing rates are maximal during the most productive season (Lyngsgaard et al., 2017). The potential grazing on phytoplankton biomass in this transition zone was ~10%/day in the winter, up to >100%/day during the summer, and averaged 54–79%/day of the phytoplankton biomass over the course of a year (Lyngsgaard et al., 2017). Grazing exerted such a strong and dynamic top-down control that variations of phytoplankton biomass were not dictated by bottom-up control via abiotic factors. Instead, they reflected subtle ecosystem imbalances between phytoplankton growth and grazing losses (Behrenfeld & Boss, 2014).

The East China Sea (ECS) lies over the world's most extensive continental shelf and has experienced a variety of environmental changes. Based on a large data set from satellites and fieldwork, our previous study has synthesized current knowledge of seasonal variations of phytoplankton biomass and community structure in the ECS (Liu et al., 2016). Seasonal fluctuations of several water masses make the ECS shelf a highly dynamic region in which the seasonal patterns of phytoplankton biomass vary from one subarea to another. In addition, Liu et al. (2016) have noted that there might be a mismatch between PP and Chla biomass. The PP over the shelf in summer averages $939 \text{ mg C} \cdot \text{m}^{-2} \cdot \text{day}^{-1}$, about 3 times the rates measured in other seasons, which are lower because of light limitation (Gong et al., 2003). This pattern differs from the seasonal variations of Chla concentrations, regardless of whether the latter are determined via remote sensing or direct measurements (Liu et al., 2016; Yamaguchi et al., 2013).

In this study, we simultaneously estimated PP, ^{15}N -based nitrate assimilation (NA), and particulate organic carbon (POC) concentrations on four cruises during different seasons in the dynamic shelf ecosystems of the ECS. To complement these data, ancillary measurements of nutrient concentrations, phytoplankton carbon biomass, Chla, and pigment-based community structure were made during the same cruises. We combined our results with previously reported simultaneous estimates of Chla, PP, and NA (Table 1). Our goal was to test the null hypothesis that there are no differences in the seasonal patterns of phytoplankton biomass and PP in the ECS. Our rejection of this hypothesis may reflect a universal phenomenon that is explained mainly by seasonal variations of C:Chla ratios (Behrenfeld et al., 2016; Jakobsen & Markager, 2016) and grazing impacts (Behrenfeld & Boss, 2014; Lyngsgaard et al., 2017). Through this study, we hoped to gain insights into the factors and processes that regulate phytoplankton communities and to better understand the dynamics of continental shelf ecosystems.

2. Materials and Methods

Four cruises were conducted as a part of the National Basic Research Programs of China (The 973 Programs: CHIOIC-C) in the ECS from August 2009 to May 2011 (Table 1). Hydrographic measurements and water samples were taken using Niskin bottles attached to a rosette sampler with a conductivity-temperature-

Table 1
Summary of Cruise Information Related to Simultaneous Measurements of Primary Production and Nitrate Assimilation in the East China Sea

No	Cruises	Year/month	Seasons	Study area/station number	Reference
1	K-92-09	1993/02	Late Winter	PN line/4	Kanda et al. (2003)
2	K-93-05	1993/10	Autumn	PN line/6	Kanda et al. (2003)
3	K-94-04	1994/08	Summer	PN line/5	Kanda et al. (2003)
4	416	1995/04	Spring	South of the ECS/3	Chen et al. (1999)
5	124	1995/06	Summer	South of the ECS/5	Chen et al. (1999)
6	431	1995/09	Early Autumn	South of the ECS/3	Chen et al. (1999)
7	SE-96-01	1996/04	Spring	PN line/3	Kanda et al. (2003)
8	449	1996/05	Late Spring	The ECS/9	Chen et al. (1999)
9	RV/OR1-493	1997/07	Summer	The ECS/8	Chen et al. (2001)
10	RV/OR1-511	1997/12	Early Winter	The ECS/9	Chen et al. (2001)
11	RV/OR1-515	1998/03	Early Spring	The ECS/9	Chen and Chen (2003)
12	RV/OR1-532	1998/10	Autumn	The ECS/9	Chen and Chen (2003)
13	RV/OR1	1998/07	Summer	The ECS/9	Chen et al. (2004)
14	CHOICE-C1	2009/08	Summer	The ECS/10	This study
15	CHOICE-C2	2009/12–2010/01	Winter	The ECS/11	This study
16	CHOICE-C3	2010/11–12	Late Autumn	The ECS/10	This study
17	KT-10-19	2010/09	Autumn	Out shelf of the ECS/3	Liu et al. (2013)
18	CHOICE-C4	2011/05–06	Late Spring	The ECS/9	This study

Note. ECS = East China Sea. The PN line is a typical section from the Yangtze Estuary to the Kuroshio area.

depth (CTD) profiler (Seabird SBE CTD 911 or 917). The samples used for determination of nutrient and Chla concentrations were collected from 3 to 8 depths within the upper 200 m of the water column, including surface water, the Chla maximum, and the bottom of the euphotic zone. The euphotic zone was defined as the water column down to a depth at which the downward flux of photosynthetically active radiation (PAR) was 1% of the value just below the surface. Vertical profiles of PAR were obtained at each station using a PAR sensor (Biospherical Instruments Inc., USA) attached to a CTD. Average values within the euphotic zone of Chla, PP, and NA were determined by trapezoidal integration using the same depths. For convenience, surface, integral, and mean values are abbreviated throughout the manuscript, such as S-Chla, I-Chla, and M-Chla, respectively.

2.1. Chla, POC, C Biomass, and Community Structure

The methods used to determine phytoplankton Chla concentrations and community structure have been previously described by Liu et al. (2016). Briefly, phytoplankton pigments were extracted in *N,N*-dimethylformamide and analyzed using an Agilent series 1100 HPLC system fitted with a 3.5- μ m Eclipse XDB C₈ column (4.6 \times 150 mm, Agilent Technologies, Waldbronn, Germany; Zapata et al., 2000). Quantification was performed with standards that were purchased from DHI Water & Environment, Hørsholm, Denmark. Based on pigment concentrations, we estimated the relative abundance of different phytoplankton groups using CHEMTAX (Mackey et al., 1996). The CHEMTAX calculations were performed using the improved procedures described by Latasa (2007). The pigment-based phytoplankton groups were classified into the following size categories: microphytoplankton (diatoms + dinoflagellates), nanophytoplankton (haptophytes + chlorophytes + cryptophytes), and picophytoplankton (*Prochlorococcus* + *Synechococcus* + prasinophytes) in accord with Uitz et al. (2006).

Based on cell abundance and carbon content, we estimated phytoplankton C biomass. Observations contemporaneous with our study for cell abundances of microphytoplankton and picophytoplankton have been published by S. J. Guo, Feng, et al. (2014) and C. Guo, Liu, et al. (2014), respectively. Samples for species and abundance analyses of diatoms and dinoflagellates were fixed with 2% buffered formalin and kept in a dark place. Phytoplankton cells were concentrated with 100-ml settling columns for 1–2 days and then identified and counted with an Olympus inverted microscope at 400X magnification (Utermöhl, 1958). Harrison et al. (2015) have determined phytoplankton cell volumes and carbon contents for 214 of the most common species found in globally distributed coastal areas, including the ECS. In addition, Chang et al. (2003) have presented cell volume and abundance data for the dominant species in 5-m depth intervals at three selected stations located in the coastal, midshelf, and Kuroshio regions of the ECS. Samples for flow

cytometric analysis were fixed with buffered paraformaldehyde (0.5% final concentration) and stored at -80°C until analysis. Abundances of autotrophic picophytoplankton (*Prochlorococcus*, *Synechococcus*, and picoeukaryotes) were enumerated using a FACS Vantage SE flow cytometer (Becton Dickinson). Phytoplankton cells were delineated on the basis of side scattering and the red/orange autofluorescence emitted by chlorophyll/phycoerythrin (Olson et al., 1993). Based on published relationships between cell size and carbon content (Chen et al., 2011; Harrison et al., 2015), we calculated the carbon biomass of diatoms, dinoflagellates, *Prochlorococcus*, *Synechococcus*, and picoeukaryotes. The total C:Chla ratios were calculated from these carbon estimates and the measured Chla concentration.

Many previous studies have compared C:Chla and POC:Chla ratios with the goal of developing simple, reasonably accurate equations for converting Chla concentrations into carbon-based biological parameters (Eppley et al., 1977; Legendre & Michaud, 1999). In this study, POC concentrations were determined in accord with U.S. Joint Global Ocean Flux Study (JGOFS) protocols using an elemental analyzer (PerkinElmer 2400 series II CHNS/O, Waltham, USA; Knap et al., 1996). Each sample was corrected for a C (or N) blank and treated via acid fuming to remove carbonates. The precision of the POC determinations was better than 10% based on replicate analyses (Cai et al., 2015).

2.2. PP and NA

The PP and NA measurements were made in the ECS during four “CHOICE-C” cruises of the R/V Dongfanghong2 during the four seasons of the year (Table 1). Details of the PP and NA measurement protocols have been described previously (Liu et al., 2013; Xie et al., 2015). The procedures were in accord with those used by Gong et al. (2003) and Chen et al. (1999), respectively. Briefly, seawater samples were collected from 3 to 5 depths (depending on the depth of the euphotic zone) from the surface to the bottom of the euphotic zone (e.g., 100%, 50%, 25%, 10%, and 1% of surface irradiance). The water was prescreened through 200- μm mesh and then added to 250-ml acid-cleaned polycarbonate bottles (Nalgene, Rochester, USA). The samples were then wrapped in neutral-density screens (LEE, London, UK) to adjust each light level to the desired irradiance. The bottles were incubated in an on-deck incubator cooled by flowing surface seawater for 4 hr. Photosynthetic carbon fixation was determined from the uptake of inorganic ^{14}C added as $\text{NaH}^{14}\text{CO}_3$ (Steemann Nielsen, 1952). Carb-Sorb E (Packard, Germany) was used to determine the total radioactivity of the samples. Before the radioactivity was counted on a Tri-Carb 2800TR liquid scintillation counter (PerkinElmer), the filters were fumed with acid to remove residual inorganic carbon and then submerged in 10 ml of Ultima Gold scintillation cocktail (Perkin Elmer) overnight. Productivity-irradiance curves were determined based on incubations conducted at nine light levels for each depth. The I-PP over the euphotic zone was calculated using a productivity-irradiance model (Xie et al., 2015).

NA rates were estimated based on 3-hr incubations conducted during the day. The samples to be incubated were collected in duplicate, acid-cleaned, 2-L polycarbonate bottles, and ^{15}N -labeled nitrate (99.21 at. % ^{15}N) was added to each bottle to give final tracer concentrations of 30–1,000 nM, depending on the ambient nitrate concentrations. The ^{15}N additions amounted to 30–100% of ambient nitrate concentrations. Samples were filtered through 25-mm GF/F filters (Whatman, $\sim 0.7\ \mu\text{m}$), and POC, particulate nitrogen, and the $^{15}\text{N}/^{14}\text{N}$ isotopic ratios were determined using an elemental analyzer (Carlo Erba NC 2500, CE, Wigan, UK) connected to a mass spectrometer (MAT DELTAplus XL, Finnigan, Ringoes, USA). The assimilation rates were calculated assuming Michaelis-Menten kinetics to correct for overestimation caused by perturbation of the ambient nitrate concentration by the ^{15}N spike (Kanda et al., 2003). This correction was especially important in nitrate-depleted surface water ($<0.1\ \mu\text{M}$). The daily results were calculated based on the ratio between the daytime and nighttime assimilation rates in a 2-year study at the Bermuda Atlantic Time Series site in the subtropical North Atlantic Ocean (Lipschultz, 2001). Nitrate-based new production (NP) in units of carbon was calculated from the NA rate and the Redfield Ratio (C:N = 6.6 atom:atom), and the f-ratio was defined as NP/PP (Dugdale & Goering, 1967; Eppley & Peterson, 1979).

The Changjiang River plume, shelf, and Kuroshio waters were defined on the basis of their surface salinities: <31 , $31\text{--}33.5$, and >33.5 , respectively (Liu et al., 2016). A one-way analysis of variance (ANOVA) was used for statistical analyses. If means were judged to be significantly different ($p < 0.05$) based on ANOVA, post hoc tests were conducted using the least significant difference criterion. If the variances were different, a nonparametric Kruskal-Wallis (KW) test based on the ranks of the data was used instead of ANOVA. Correlations between two variables were tested for significance using a Spearman rank correlation

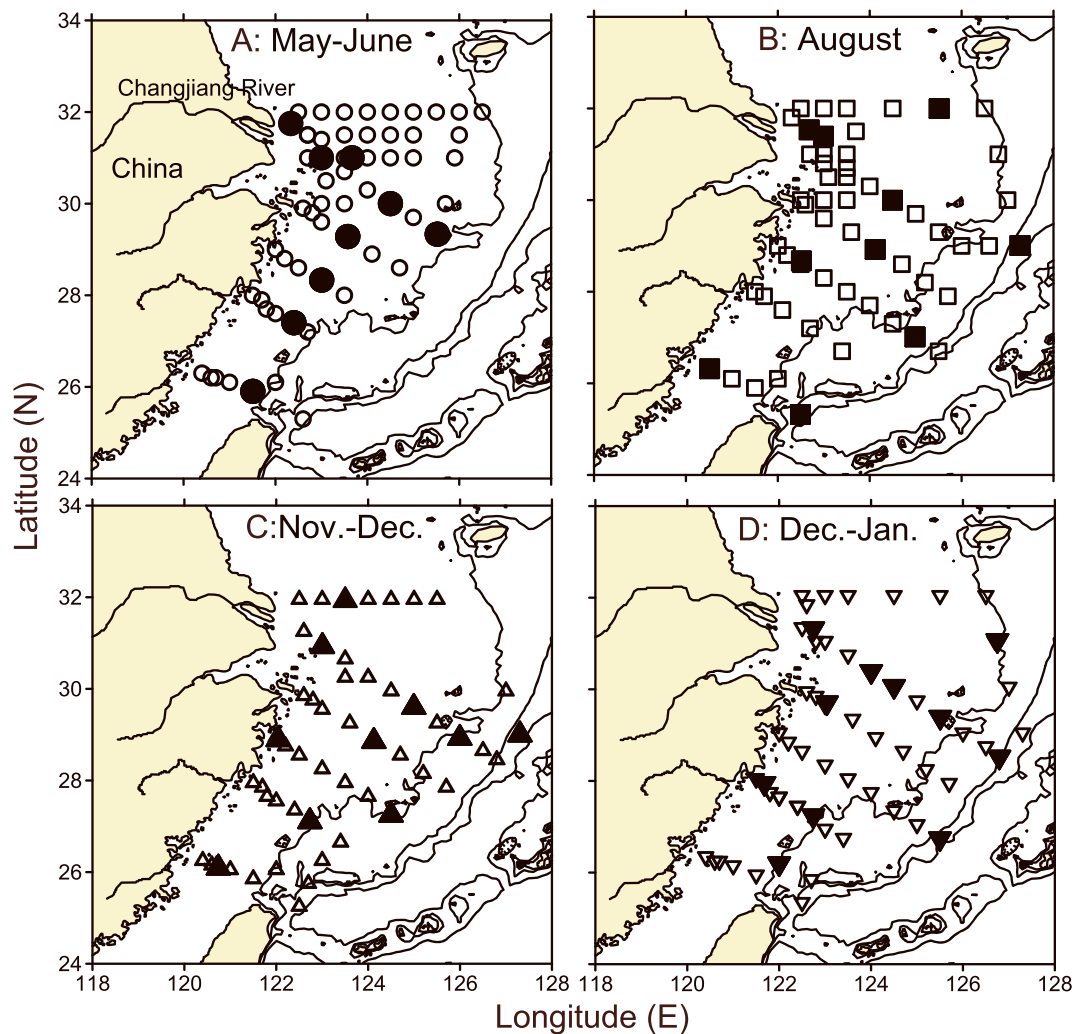


Figure 1. Map of sampling stations in the East China Sea during cruises CHOICE C1–C4 of different seasons (a–d indicate results during four cruises of CHOICE C1–C4 in the Table 1), with isobaths of 100, 200, and 1,000 m. Open icons denote stations of measuring temperature, salinity, nutrients, and chlorophyll concentration and solid icons indicating primary and new production measurement stations.

coefficient (R_S) to avoid artifacts when data did not appear to be normally distributed (Anscombe, 1973). All statistical tests were conducted using statistical packages for social sciences software (SPSS 16.0). To contrast the overall seasonal difference in S-Chla, I-PP, and I-NP, we used a generalized linear mixed-effects model using salinity (water mass) as a random effect with the lme4 package for R (Bates et al., 2015). The significance level was set at $p < 0.05$. Linear functions were normally used to describe the relationship between I-PP and S-Chla concentrations and between I-PP and I-NA rates during the four CHOICE cruises (C1–C4) and all cruises in Table 1. Because the estimates of the slope and intercept from ordinary least squares regression are biased when the independent variable is uncontrolled (Laws et al., 2016), the linear regressions were conducted using the Model II geometric mean method with the package “lmodel2” of R software (R Core Team, 2016).

3. RESULTS

3.1. Seasonal Variations

PP and NA were measured at 9, 10, 10, and 11 stations during the cruises in late spring, summer, late autumn, and winter, respectively (Figure 1). There were large seasonal and spatial variations of the euphotic zone I-PP and I-NA (Figures 2 and 3). The ranges of I-PP during May–June, August, November–December, and December–January were 87–5,327, 167–3,710, 92–1,005, and 72–896 $\text{mg C}\cdot\text{m}^{-2}\cdot\text{day}^{-1}$, respectively. The

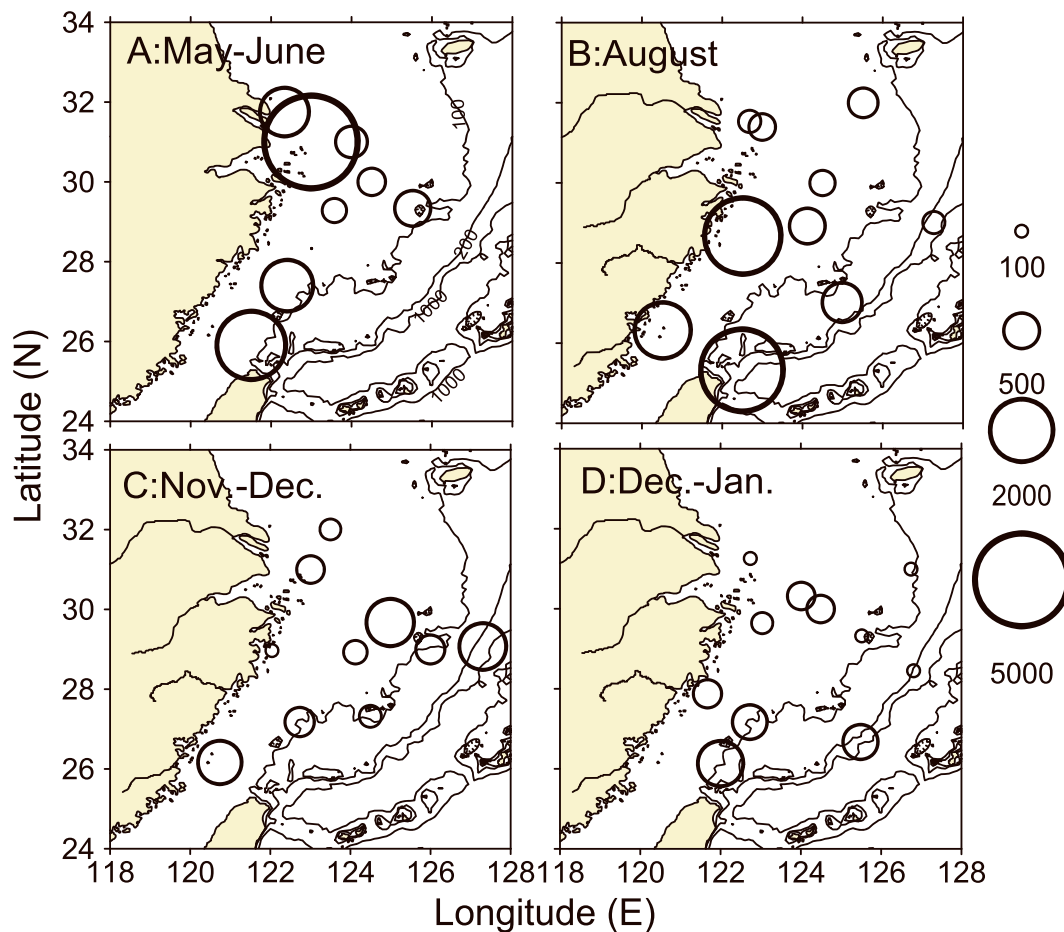


Figure 2. The spatial variations on the water column integrated primary production ($\text{mg C}\cdot\text{m}^{-2}\cdot\text{day}^{-1}$) of different seasons (a-d indicate results during four cruises of CHOICE C1–C4 in the Table 1), with isobaths of 100, 200, and 1,000 m.

maximum I-PP ($5,327 \text{ mg C}\cdot\text{m}^{-2}\cdot\text{day}^{-1}$; Figure 2a) occurred in June at Station PN10 near the Changjiang (Yangtze) River estuary, where the S-Chla concentration reached $25.5 \text{ mg}/\text{m}^3$ during a bloom of *Prorocentrum dentatum*. Outside the Changjiang estuary in August, the I-PP rates were only 170 and $244 \text{ mg C}\cdot\text{m}^{-2}\cdot\text{day}^{-1}$ (Figure 2b).

The range of the I-NA was $2\text{--}417 \text{ mg N}\cdot\text{m}^{-2}\cdot\text{day}^{-1}$, and the distributions were generally consistent with those of PP ($R_S = 0.56$, $n = 38$, $p < 0.01$; Table 2). The average f-ratio was 0.46 (Figure 4b). The NA rates decreased gradually from the inner shelf to the outer shelf in warm seasons and from south to north during cold seasons (Figure 3). I-PPs were positively correlated with S-Chla concentrations (Table 2 and Figure 4a), but the R_S was only 0.38. The corresponding R_S values between I-PP and I-Chla concentrations were not significant (Table 2).

Combined with the results of published studies (Table 1), the mean I-PP in all stations during summer was $1.15 \pm 1.19 \text{ g C}\cdot\text{m}^{-2}\cdot\text{day}^{-1}$ (mean \pm SD, $n = 40$), 3 times the mean rate in winter ($0.41 \pm 0.32 \text{ g C}\cdot\text{m}^{-2}\cdot\text{day}^{-1}$; Figure 5b). The overall M-PP measured in late autumn and winter were significantly lower than the M-PP measured in summer (KW Test, Table 3). The seasonal pattern of NP was similar to that of PP ($R_S = 0.70$, $n = 117$, $p < 0.01$, Table 2), with significantly higher values in summer ($0.51 \pm 0.65 \text{ g C}\cdot\text{m}^{-2}\cdot\text{day}^{-1}$) than in winter ($0.14 \pm 0.15 \text{ g C}\cdot\text{m}^{-2}\cdot\text{day}^{-1}$, KW Test, Table 3 and Figure 5c). These patterns differed from the seasonal variations of the Chla concentrations, which were highest in the spring but lowest in the summer (KW Test, Table 3), when PP and NA were high. We also noted that there was more than a 100-fold range of Chla concentrations during the summer, an indication of great spatial variability (Figure 5a). In summer, the

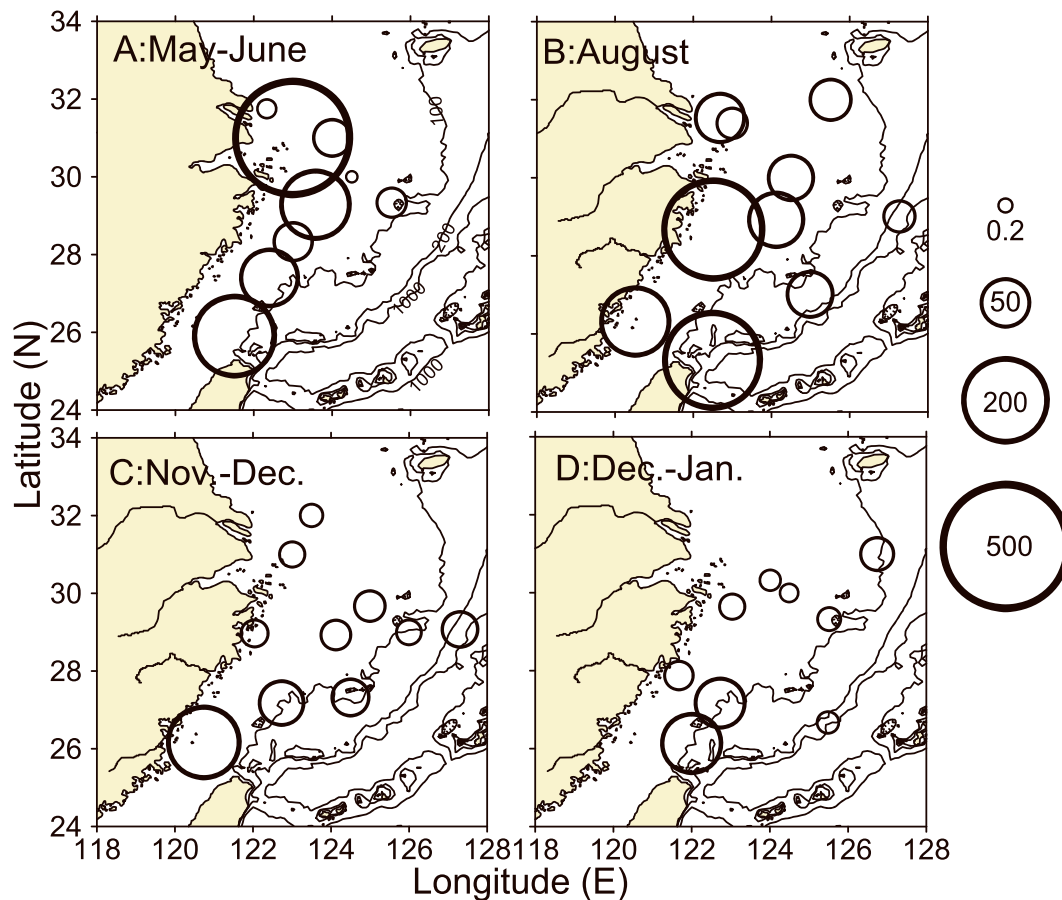


Figure 3. The spatial variations on the water column integrated nitrate assimilation ($\text{mg N}\cdot\text{m}^{-2}\cdot\text{day}^{-1}$) of different seasons (a–d indicate results during four cruises of CHOICE C1–C4 in the Table 1), with isobaths of 100, 200, and 1,000 m.

Chla concentrations were high in coastal waters because of nutrient inputs from rivers and upwelling but very low in off-shelf waters because of strong stratification.

We used a generalized linear mixed-effect model using salinity (water mass) as a random effect to contrast the overall seasonal differences in S-Chla, I-PP, and I-NP (Table 3). The results showed that if spatial variations were eliminated, there was no significant variation of Chla concentrations between summer and winter. However, PP and NP were significantly higher in summer than in autumn and winter (Table 3).

We examined in detail the seasonal variations in the different water masses (Table 4). In the plume and middle shelf waters, the seasonal variations of M-Chla concentrations were in phase with those of PP. The highest M-Chla concentration ($5.18 \mu\text{g/L}$) and I-PP ($2.11 \text{ g C}\cdot\text{m}^{-2}\cdot\text{day}^{-1}$) in the plume were observed during the spring. The corresponding values of I-PP in shelf waters were highest in summer and were associated with relatively high Chla concentrations. However, the seasonal variations of Chla were out of phase with the variations of PP in off-shelf waters, where the highest M-PP ($0.83 \text{ g C}\cdot\text{m}^{-2}\cdot\text{day}^{-1}$) was associated with the lowest S-Chla concentration ($0.31 \mu\text{g/L}$), both of which were measured in the summer.

3.2. Relationships With Community and Size Structure

The phytoplankton communities in the ECS were dominated by microphytoplankton and/or nanophytoplankton (Figure 6a). Their contributions to Chla varied widely, from $<30\%$ in the off-shelf waters to $>70\%$ in the coastal area. Picophytoplankton contributed mainly in the surface off-shelf waters during the summer, but their contribution was still less than 50% (mostly less than 30%) of the I-Chla in all the samples. The two highest Chla concentrations were accounted for primarily by microphytoplankton ($>80\%$) and were associated with algal blooms that occurred in the spring and autumn. During the spring, high Chla concentrations were the result of a dinoflagellate bloom, whereas in autumn, diatoms dominated.

Table 2
Spearman Correlation Coefficients (R_S), Significance Levels (p), and Samples Numbers (N) Between the Main Parameters During Cruises CHOICE C1–C4 (A) and all cruises in Table 1 (B)

Data	Parameters		NA	S-Chla	I-Chla
A	PP	R_S	0.56**	0.38*	0.23
		p	<0.01	<0.05	0.16
		N	38	38	37
	NA	R_S		0.16	0.18
		p		0.32	0.13
		N		39	38
	S-Chla	R_S			0.30**
		p			<0.01
		N			39
B	PP	R_S	0.70**	0.41**	
		p	<0.01	<0.01	
		N	117	117	
	NA	R_S		0.34**	
		p		<0.01	
		N		118	

Note. PP = integrated primary production; NA = integrated nitrate assimilation, S-Chla = surface chlorophyll a concentrations; I-Chla = integrated chlorophyll a concentrations.

*Correlation is significant at the 0.05 level. **Correlation is significant at the 0.01 level.

Although microphytoplankton usually accounted for the majority of the high Chla concentrations, the relationship between Chla concentrations and community structure was not a simple linear relationship, and in some cases, high Chla concentrations were associated with phytoplankton communities dominated by nanophytoplankton during autumn and spring (more than 50%). Seasonal variations of Chla concentrations were different in communities dominated by nanophytoplankton; in those communities, the lowest Chla concentrations were observed in summer.

Ternary plots of PP and NA (Figure 6) were similar, but there were some obvious differences with the ternary plot of Chla. During the summer, there were two high PP and NA patches, both of which were associated with low Chla concentrations. One was dominated by microphytoplankton (>80%) and the other by nanophytoplankton (~70%). Patches were also observed during late autumn and winter, but those patches were characterized by high Chla concentrations and low PP rates.

3.3. Variations of C:Chla and f-Ratios in Different Water Masses

Based on cell abundance and carbon content, the mean carbon biomasses of diatoms and dinoflagellates in surface waters were 18.9 and 12.7 $\mu\text{g C/L}$, respectively. Consistent with the pigment analyses, they were the two dominant groups in the ECS, especially in coastal areas. The mean

carbon biomasses of *Prochlorococcus*, *Synechococcus*, and picoeukaryotes in surface waters were lower by roughly an order of magnitude: 0.57, 2.27, and 3.50 $\mu\text{g C/L}$, respectively.

The ratios of phytoplankton carbon to total Chla in both summer and winter were relatively stable in the plume and shelf waters, where they averaged about 30 (Figure 7a). In contrast, the significantly higher corresponding ratios in off-shelf waters during the summer than winter suggested that the Chla-normalized carbon biomass was higher in summer. This conclusion is consistent with the high values of the Chla

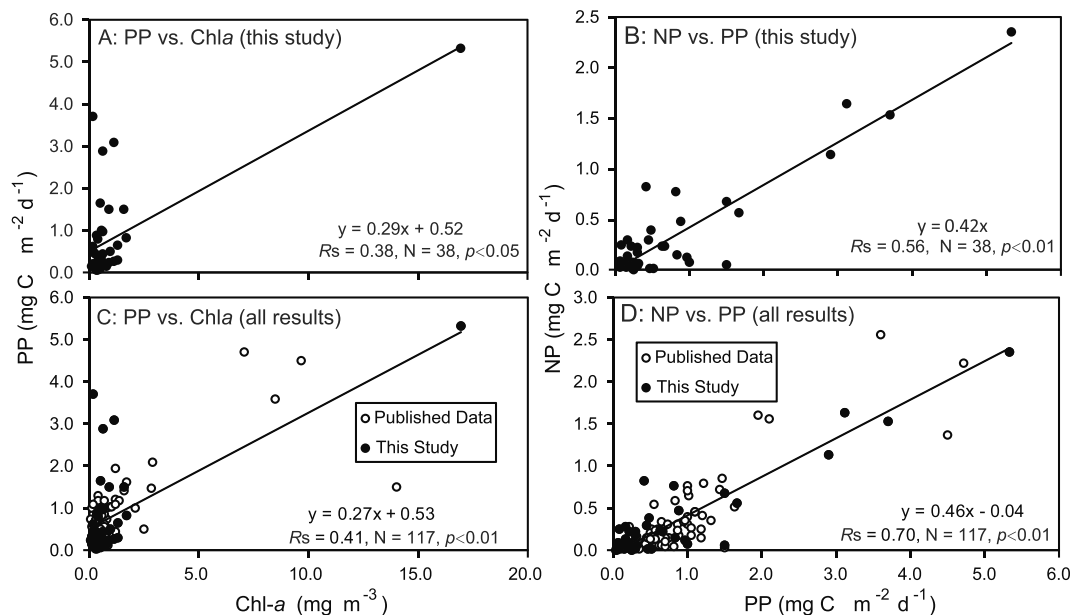


Figure 4. The relationship between integrated primary production (PP, $\text{mg C m}^{-2} \text{day}^{-1}$) and (a and c) surface chlorophyll a concentrations (Chla, mg/m^3) and (b and d) integrated new production (NP, $\text{mg C m}^{-2} \text{day}^{-1}$) during four cruises of CHOICE C1–C4 (a and b) and all cruises in the Table 1 (c and d). Nonparametric Spearman correlation coefficient (R_S) is significant (p) at the 0.05 or 0.01 level (two-tailed).

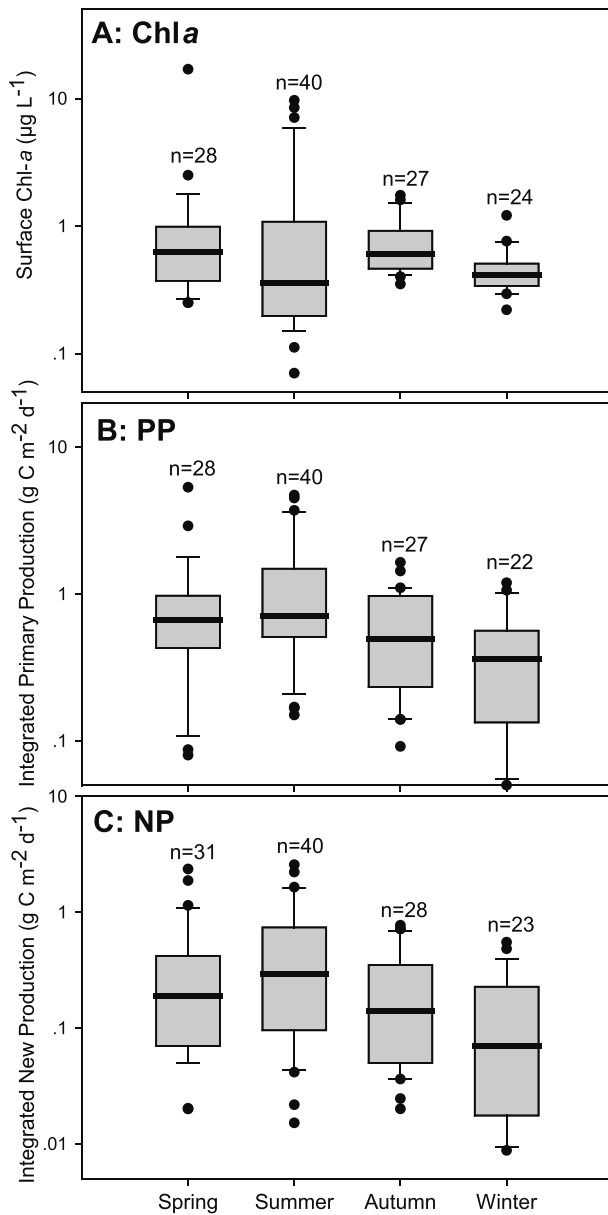


Figure 5. Seasonal variations of (a) surface chlorophyll *a* concentrations (Chla, $\mu\text{g/L}$), (b) integrated primary production (PP, $\text{g C m}^{-2}\cdot\text{day}^{-1}$), and (c) integrated new production (NP, $\text{g C m}^{-2}\cdot\text{day}^{-1}$) in the East China Sea. Numbers on the box are the sample number during all cruises in the Table 1.

during the spring bloom is limited by the low Chla-normalized production rate of *Phaeocystis* sp., a reflection of the low temperatures at that time of year (Barnes et al., 2015; Xie et al., 2015). Lyngsgaard et al. (2017) have reported Chla concentrations in the Baltic Sea transition zone during the spring are higher than at other times of year, whereas C and PP are much lower in spring than in summer. In the southern Bay of Biscay, different seasonality of Chla and C biomass resulted in a clear temporal pattern of picophytoplanktonic C:Chla ratios, which ranged from 10 in winter to 140 in summer (Calvo-Díaz et al., 2008). The similarity of these patterns in the ECS, the Western English Channel, the Baltic Sea, and the Bay of Biscay indicates that Chla is not a good indicator for PP, particularly during the summer, and it is often not a good proxy for phytoplankton C biomass either. This lack of correlation between Chla and both PP and C may be a global phenomenon and, if so, further challenge satellite-based estimates of global C biomass and PP from Chla.

normalized PP (PP/Chla) in the off-shelf area during summer (Table 4). Despite the very significant correlation between PP and NP (Table 3), the f-ratios (NP/PP) were generally lower in the coastal region (especially the plume, Table 4) than in off-shelf waters.

Because of the uncertainty in the calculated phytoplankton carbon biomass, we calculated POC:Chla ratios at the same times. Those ratios were also significantly higher during the summer (Figure 7b). However, POC:Chla ratios were as much as 2–3 times C:Chla, ratios, and there was no significant difference between coastal and off-shelf POC:Chla ratios in the summer.

4. Discussion

4.1. Uncoupling Between Chla and PP

Our results indicate that I-PP was correlated with S-Chla concentrations, but no significant correlation was found with I-Chla values (Table 2). This result is not surprising, because the vertical distributions of PP and Chla differ. The maximum of PP tends to occur at the surface or, because of photoinhibition (Behrenfeld & Falkowski, 1997), just below the surface (about 50% of surface PAR). However, the Chla maximum is typically found deep in the euphotic zone and sometimes as deep as 100 m in oligotrophic areas (Cullen & Eppley, 1981). As indicated by Behrenfeld and Falkowski (1997), the modeled PP could explain more than 80% of the variability in the measured values, because the optimal production usually occurred in the near-surface location, and previous studies have pointed out that Chla at a depth within the euphotic zone is a function of Chla at the surface in most instances (Morel & Berthon, 1989; Uitz et al., 2006). A similar relationship in the ECS would imply that a depth-integrated PP model like Vertically Generalized Production Model (VGPM) using satellite data could be applied successfully.

Our results indicated that the phytoplankton C:Chla ratios in off-shelf waters were significantly higher during summer (Figure 7a). This pattern is consistent with the high photosynthetic rates normalized to Chla (PP/Chla) in the off-shelf area during the summer (Table 4). Our results also suggested that the increase of Chla concentrations preceded the increase of PP rates in coastal waters, but in off-shelf areas, the seasonal variations of Chla were completely out of phase with the variations of PP (Figure 8b). A similar seasonal pattern of Chla and PP has been observed in the temperate Western English Channel (Xie et al., 2015), Danish waters (Jakobsen & Markager, 2016; Lyngsgaard et al., 2017), and the Cantabrian Sea (Calvo-Díaz et al., 2008). In the Western English Channel, although the Chla concentrations are high in the spring, PP

Table 3

Sample Number (N) and Significance Levels (p) of Overall Seasonal Differences in the East China Sea on Surface Chlorophyll a Concentration (Chla), Integrated Primary Productivity (PP) and New Production (NP), Used Kruskal-Wallis Test, and a Generalized Linear Mixed-Effect Model (GLMM) Using Salinity (Water Masses) as a Random Effect During All Cruises in Table 1

Seasons	N	Kruskal-Wallis			GLMM		
		Mean Rank	Chi-Square	Sig.	Summer	Autumn	Winter
Chla							
Spring	28	72.89			0.57	0.58	0.21
Summer	40	47.51				0.74	0.27
Autumn	27	73.76					0.01*
Winter	24	50.29					
Total	119		15.51	0.001**			
PP							
Spring	28	61.07			0.39	0.04*	0.08
Summer	40	69.22				0.05*	0.01*
Autumn	27	56.87					0.12
Winter	22	40.39					
Total	117		10.54	0.014*			
NP							
Spring	31	67.56			0.14	0.01*	0.08
Summer	40	69.82				0.02*	0.01*
Autumn	28	58.77					0.18
Winter	23	42.17					
Total	122		10.49	0.015*			

*Correlation is significant at the 0.05 level. **Correlation is significant at the 0.01 level.

4.2. Variations of C:Chla Ratios

The uncoupling can be attributed mainly to the phytoplankton community's response to environmental changes, especially the combined effects of variations of light, nutrient availability, and temperature, on the seasonal patterns of C:Chla ratios. Behrenfeld et al. (2016) have shown that physiological changes in cellular

Table 4

Definitions of Surface Water Masses (≤ 5 m) in the East China Sea During All Cruises in Table 1

Water masses	S	N	Temp	Sal	Bot.	Ze	PP	NP	f	Chla	PP/Chla	NP/Chla
Plume	S	4	16.5 (2.8)	30.2 (0.5)	41 (13)	19 (11)	2.11 (2.19)	0.59 (1.00)	0.25 (0.18)	5.18 (7.85)	0.67 (0.29)	0.14 (0.12)
	S	10	26.2 (2.3)	28.6 (1.9)	46 (12)	18 (10)	1.84 (1.67)	0.68 (0.80)	0.35 (0.20)	3.79 (4.80)	1.03 (0.93)	0.38 (0.44)
	A	3	17.7	29.9	16	20	0.47 (0.47)	0.31 (0.35)	0.60 (0.10)	1.07 (0.89)	0.39 (0.19)	0.37 (0.23)
	W	4	14.1 (1.3)	30.1 (0.4)	40 (5)	12 (6)	0.21 (0.19)	0.06 (0.06)	0.24 (0.06)	0.65 (0.38)	0.30 (0.22)	0.08 (0.05)
Shelf water	S	7	17.9 (3.3)	32.8 (0.5)	64 (22)	32 (10)	0.61 (0.27)	0.37 (0.61)	0.31 (0.20)	0.92 (0.46)	0.69 (0.35)	0.20 (0.14)
	S	12	26.8 (2.2)	32.9 (0.6)	88 (33)	54 (27)	1.07 (0.94)	0.53 (0.77)	0.43 (0.25)	1.22 (2.41)	2.74 (2.73)	1.13 (1.29)
	A	6	23.5 (3.5)	32.7 (0.8)	81 (76)	12 (7)	0.63 (0.61)	0.21 (0.23)	0.25 (0.11)	1.02 (0.43)	0.57 (0.40)	0.11 (0.13)
	W	3	16.1 (3.2)	32.6 (0.8)	53 (39)	20 (21)	0.36 (0.28)	0.10 (0.08)	0.30 (0.07)	0.49 (0.19)	0.65 (0.46)	0.19 (0.16)
Off-shelf water	S	17	20.0 (3.0)	34.2 (0.3)	155 (244)	60 (19)	0.72 (0.69)	0.34 (0.32)	0.60 (0.72)	0.61 (0.53)	1.47 (1.27)	0.63 (0.52)
	S	18	26.8 (2.5)	34.0 (0.3)	171 (145)	64 (28)	0.83 (0.88)	0.39 (0.47)	0.52 (0.39)	0.31 (0.34)	3.69 (4.17)	1.29 (0.63)
	A	18	23.0 (1.9)	34.1 (0.3)	117 (114)	52 (19)	0.67 (0.38)	0.24 (0.22)	0.40 (0.27)	0.66 (0.35)	1.16 (0.67)	0.42 (0.44)
	W	15	19.6 (2.9)	34.2 (0.3)	201 (279)	49 (28)	0.47 (0.35)	0.16 (0.17)	0.40 (0.39)	0.43 (0.14)	0.99 (0.89)	0.33 (0.36)

Note. Samples of different seasons are arranged in the order spring, summer, autumn, and winter (S, S, A, and W, respectively), with comparisons of their sample number (N) of simultaneous measurements, means, and standard deviations (in parentheses) of surface temperature (Temp, °C), salinity (Sal), station bottom depth (Bot., m), euphotic zone depth (Ze, m), integrated primary production (PP, mg C·m⁻²·day⁻¹) and new production (NP, mg C·m⁻²·day⁻¹), f-ratios (NP/PP), surface chlorophyll a concentration (Chla, µg/L), and ratios of PP and NP to Chla.

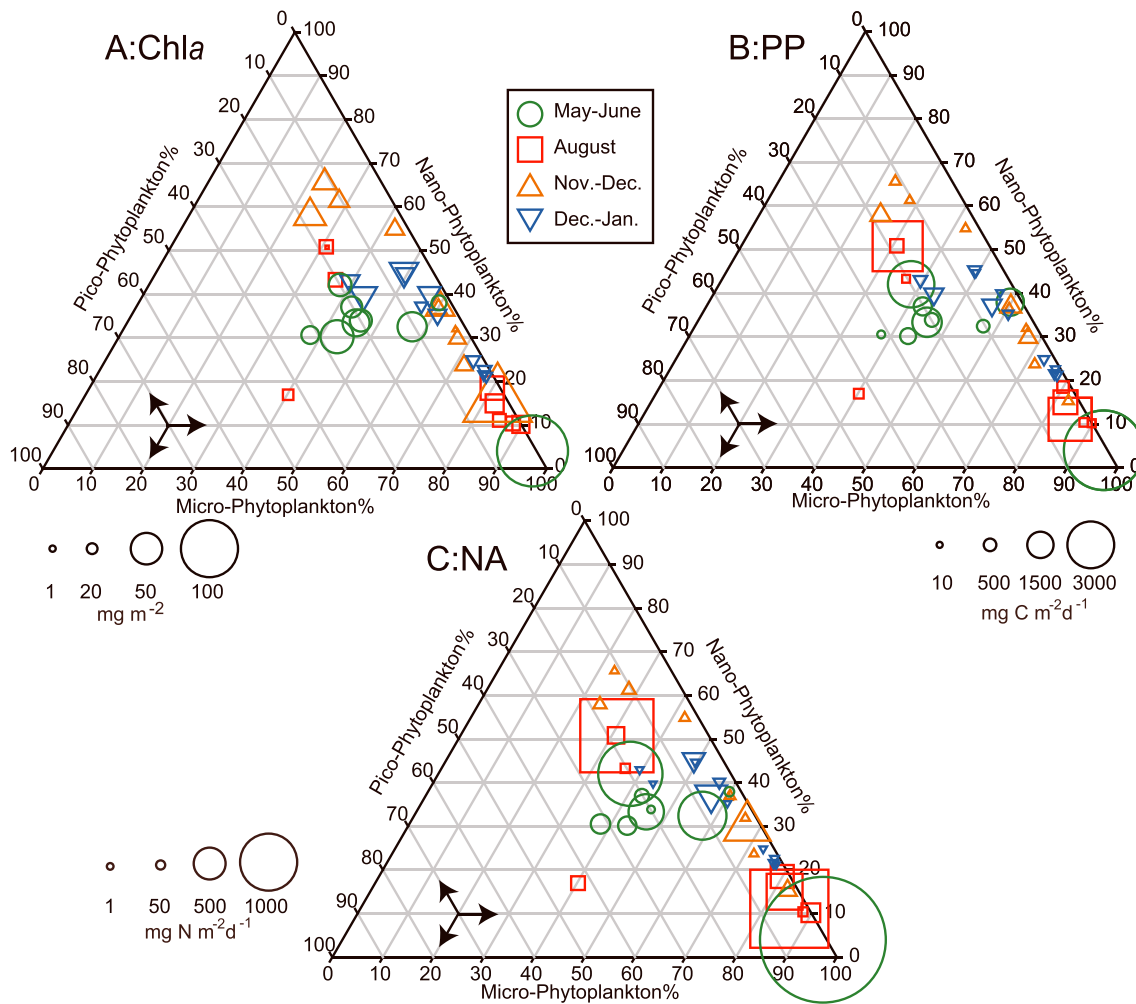


Figure 6. The ternary plot of (a) seasonal integrated chlorophyll *a* (Chla, mg m^{-2}), (b) integrated primary production (PP, $\text{mg C m}^{-2} \cdot \text{day}^{-1}$), and (c) integrated nitrate assimilation (NA, $\text{mg N m}^{-2} \cdot \text{day}^{-1}$) as function of phytoplankton community structure (relative abundance of different groups on Chla biomass) during four cruises of CHOICE C1–C4 (Table 1).

pigmentation are often responses to changing mixed-layer light conditions (photoacclimation). Controlled laboratory experiments have shown that phytoplanktons increase their Chla concentrations under low-light conditions to maximize light absorption (Beardall & Morris, 1976; Falkowski & Owens, 1980), whereas under high-light conditions, they tend to accumulate more carbon, and C:Chla ratios increase (Terry et al., 1983). Jakobsen and Markager (2016) have also stated that changes of C:Chla ratios in Danish waters are due mainly to physiological acclimations induced by seasonal changes of irradiance and nutrient (nitrogen) availability, in the latter case especially during the period of water column stratification in the summer.

Indeed, the supply of nutrients affects the C:Chla ratio, which increases and decreases under nitrogen-limited and nitrogen-replete conditions, respectively (Geider et al., 1997). The decline of photosynthetic rates normalized to Chla in the oligotrophic subtropical gyres is presumably due to nutrient limitation (Behrenfeld & Falkowski, 1997). Marañón et al. (2003) have also indicated that PP rates in the subtropical Atlantic gyre are not associated with variations in incident surface irradiance, chlorophyll concentrations, phytoplankton C biomass, or size structure but rather with the rate of nutrient supply to the euphotic zone. A previous study of the ECS has shown that surface C:Chla ratios during summer are higher in the outer-shelf oligotrophic waters than the nutrient-rich coastal waters (Chang et al., 2003). In addition, laboratory studies have suggested that PP normalized to Chla should be positively correlated with temperature within the ecologically relevant range of temperatures, although the empirical equation reported by Behrenfeld and Falkowski (1997) indicates that they reach a maximum on a global scale at a temperature of 20 °C (Eppley, 1972).

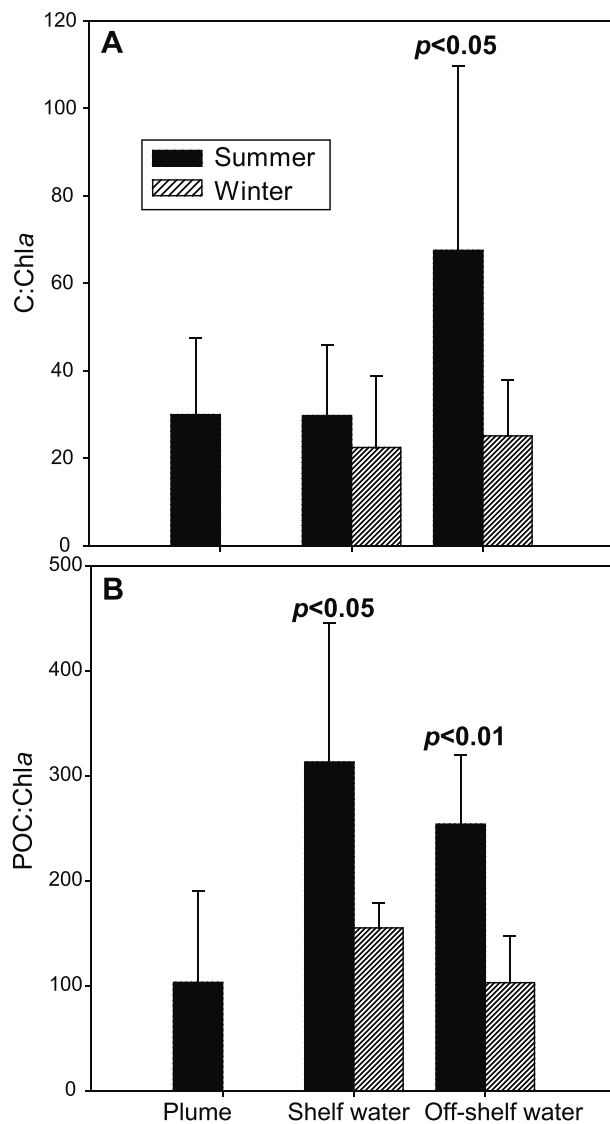


Figure 7. The ratios of (a) phytoplankton carbon biomass and (b) particulate organic carbon (POC) to chlorophyll *a* (Chla) concentrations in different water masses during summer and winter cruises in CHOICE C1 and C2. Definitions of surface water masses were shown in the Table 4. The *p* values (significant levels) on the column show the results of variance analysis.

which were high in surface waters and in summer (Table 4). Our results indicate that the increase of Chla concentrations in coastal waters preceded the increase of PP rates (Figure 8a). The explanation may be that the increase of microzooplankton grazing lags behind that of phytoplankton growth. The result would lead to positive net community productivity in the early spring and an accumulation of biomass. By summer, despite high PP, higher grazing pressure (grazing rate/growth rate) reduces the Chla concentration (Zheng et al., 2015).

In the off-shelf region, the pattern between Chla and PP was different (Figure 8b). Temperature in summer was significantly higher than in winter. Temperature would be expected to affect both rates, but grazing rates should be more sensitive to temperature than phytoplankton growth rates (Chen et al., 2012). The higher impact of grazing in summer may therefore have been caused by a greater increase of microzooplankton grazing versus phytoplankton growth rates. Although the nutrient concentrations were low in the off-shelf region during summer, microzooplankton excretion may have contributed a substantial part of the nutrient supply for the phytoplankton (Landry, 1993), but this contribution is difficult to quantify directly.

Our results are consistent with previous laboratory and open-ocean studies that have revealed how C:Chla ratios vary so as to balance the rates of the light and dark reactions of photosynthesis in response to changes of light, nutrient supplies, and temperature (Laws & Bannister, 1980; Laws & Chalup, 1990; Shuter, 1979). In fact, it is the combination of high irradiance, high temperature, and low nutrient supply rate during summer that causes Chla-normalized PP rates to be high. Those high rates are associated with high C:Chla ratios. Variations of the amplitudes of the C:Chla ratio cycles between regions reflect overall offsetting responses to changing environmental conditions (Behrenfeld et al., 2016).

We also found that there was great uncertainty in the estimation of phytoplankton biomass based on cell volume because of differences in geometric shape, especially for cells with a complex shape, and the carbon per cell volume (carbon density). In this study, our use of the average cell volume for each species led to an underestimation of seasonal differences because we overlooked the changes in cell volume associated with variations of environment factors such as temperature and nutrients. In addition, we observed a limited number of phytoplankton species under the microscope; small and nondominant species were omitted. The seasonal variations of C:Chla and POC:Chla were similar in shelf and off-shelf waters (Figure 7). The POC concentrations were roughly 5–10 times the C concentrations because the former included detritus as well as heterotrophs such as zooplankton and bacteria, whereas C values were based on microscopic measurements of phytoplankton only.

4.3. Grazing Impact

In the absence of variations of C:Chla ratios, top-down control by microzooplankton grazing would explain the mismatch between biomass and productivity, because most of the daily production of phytoplankton can be consumed by microzooplankton (Calbet & Landry, 2004). Zheng et al. (2015) have indicated that the mean rates of phytoplankton growth ($0.77 \pm 0.53 \text{ day}^{-1}$) and microzooplankton grazing ($0.69 \pm 0.42 \text{ day}^{-1}$) in summer are significantly higher than the analogous rates in winter ($0.39 \pm 0.18 \text{ day}^{-1}$ and $0.21 \pm 0.08 \text{ day}^{-1}$, respectively). Similarly, microzooplankton also consume 60–70% of the daily production by picophytoplankton, particularly in summer (C. Guo, Liu, et al., 2014). All these studies indicate that phytoplankton growth and microzooplankton grazing rates are significantly higher in summer than in winter.

The seasonal variations of phytoplankton growth rates are consistent with the seasonality of photosynthetic rates normalized to Chla (PP/Chla),

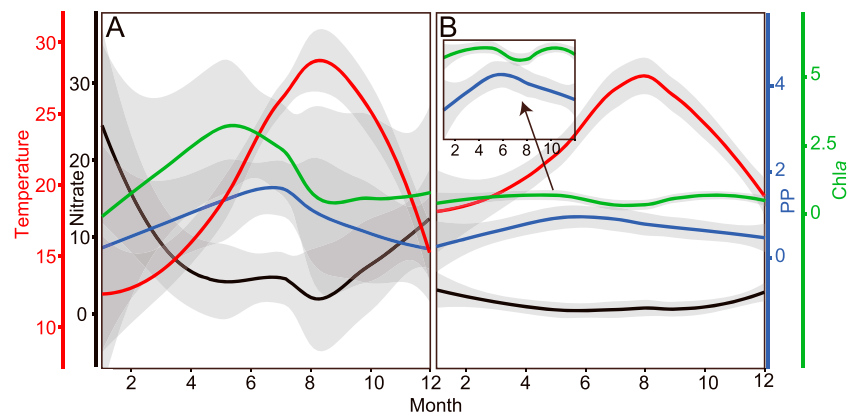


Figure 8. The schematics of seasonal variations on temperature (°C), nitrate (µM/L), chlorophyll *a* (Chla, µg/L) concentration, and primary production (integrated PP, g C·m⁻²·day⁻¹) in the plume and shelf waters (a, Salinity < 33.5) and off-shelf (b, Salinity > 33.5) areas. To smooth the data, we used R, and the solid line and shadows indicate the average and 95% confidence interval. The small box in (b) is the diagram of PP and Chla enlarging scale in the off-shelf water.

4.4. Relationships Between PP and NA

NA is also affected by light, nutrients, and temperature. Although the mechanisms are different for NA and PP, the effects of environmental factors are similar. High light, temperature, and high nutrient concentrations within a certain range can significantly increase both C and N uptake rates. Thus, there is a significant positive correlation between PP and NP in our data set and the published literature (Table 1; $R_S = 0.56$ and 0.70 , $n = 38$ and 117 ; Figure 4). They were much higher than the analogous correlations between PP and Chla concentrations (Table 2). However, the *f*-ratio may not be affected by grazing pressure as much as Chla. Our results showed that *f*-ratios changed from 0.1 (coastal area) to very close to 1 at some sites in the upwelling area northeast of Taiwan. In the Changjiang River plume, a few stations were characterized by relatively low NA but high PP, and the *f*-ratio in all seasons except autumn was smaller in the Changjiang River plume than in Kuroshio Current water (Table 3). It may seem surprising that the *f*-ratio was relatively low in an area where nutrient concentrations and PP were relatively high.

There is, however, a nontrivial amount of new nitrogen entering the ECS from the Changjiang River in the form of ammonium. Previous studies have revealed a concentration of ammonium in the Changjiang River of 14.6 µM, about half the average concentration of nitrate in runoff (Liu et al., 2009; Zhang, 1996). Therefore, the low *f*-ratio in the plume may be attributable to the negative effect of ammonium on NA. That effect can be divided into two quite distinct mechanisms, preference for ammonium and inhibition of nitrate uptake by ammonium (Dortch, 1990; Flynn et al., 1997). In any case, the ammonium in the Changjiang River is new nitrogen for the ECS, and NA may be a misleading metric of NP in such ecosystems. In addition, a large percentage of nitrate taken up may be nitrate that was recycled on the shelf as a result of ammonification followed by nitrification (Dore & Karl, 1996; Yool et al., 2007). Therefore, although variations of PP in the ECS are driven largely by nitrate uptake, nitrate is by no means the only source of new nitrogen in this dynamic ecosystem.

5. Conclusions

The present study focused on the similarities and differences of the seasonal variations of phytoplankton Chla, C biomass, PP, and NA. Some valuable insights were obtained by considering the effects of environmental factors and microzooplankton grazing on these metrics of biomass and production. Surface Chla concentrations were more highly correlated with integrated PP than with integrated Chla. The seasonal pattern of phytoplankton Chla biomass did not match that of PP, and the relationship between Chla and PP varied widely between different water masses. Significantly higher phytoplankton C:Chla ratios driven by environmental factors (light, nutrients, and temperature) were observed in the off-shelf waters during the summer. We suggest that the uncoupling of seasonal patterns of Chla and PP in the ECS was associated mainly with the seasonal variations of phytoplankton C:Chla ratios and prey-predators dynamics. Similar

patterns have been reported, and this may be an important global feature which indicates uncertainties in estimates of global satellite-based C biomass and PP from Chl_a.

Acknowledgments

This work was supported by grants of the National Key R&D Program of China (2016YFA0601201 and 2017YFC1404402), the National Basic Research Program of China (2015CB954002), the National Natural Science Foundation of China (NSFC 41776146, 41406143, and U1606404), and Xiamen University Presidential Fund (202020180102). The authors would like to thank the captain and crew of the RV “Dongfanghong 2,” who made concerted efforts to assist during field sampling. We thank Professor Pinghe Cai of Xiamen University for providing particulate organic carbon data. We also thank the chief scientist Minhan Dai for organizing the cruises and Jianyu Hu for providing the CTD data. We thank editor and reviewers for comments and suggestions on the manuscript. All data of the present study can be found by the National Key R&D Program of China “Marine Carbon Sequestration: Multiscale Regulation and Response to the Global Chang” (MARCO, <http://marco2016.xmu.edu.cn/>), or please contact Professor Huang (bqhuang@xmu.edu.cn) if any questions.

References

Anscombe, F. J. (1973). Graphs in statistical analysis. *The American Statistician*, 27(1), 17–21.

Barnes, M. K., Tilstone, G. H., Suggett, D. J., Widdicombe, C. E., Bruun, J., Martinez-Vicente, V., & Smyth, T. J. (2015). Temporal variability in total, micro- and nano-phytoplankton primary production at a coastal site in the Western English Channel. *Progress in Oceanography*, 137, 470–483. <https://doi.org/10.1016/j.pocean.2015.04.017>

Bates, D., Mächler, M., Bolker, B., & Walker, S. (2015). Fitting linear mixed-effects models using lme4. *Journal of Statistical Software*, 67(1). <https://doi.org/10.18637/jss.v067.i01>

Beardall, J., & Morris, I. (1976). The concept of light intensity adaptation in marine phytoplankton: Some experiments with *Phaeodactylum tricorutum*. *Marine Biology*, 37(4), 377–387. <https://doi.org/10.1007/BF00387494>

Behrenfeld, M. J., & Boss, E. S. (2014). Resurrecting the ecological underpinnings of ocean plankton blooms. *Annual Review of Marine Science*, 6(1), 167–194. <https://doi.org/10.1146/annurev-marine-052913-021325>

Behrenfeld, M. J., & Falkowski, P. G. (1997). Photosynthetic rates derived from satellite-based chlorophyll concentration. *Limnology and Oceanography*, 42(1), 1–20. <https://doi.org/10.4319/lo.1997.42.1.0001>

Behrenfeld, M. J., O'Malley, R. T., Boss, E. S., Westberry, T. K., Graff, J. R., Halsey, K. H., et al. (2016). Reevaluating ocean warming impacts on global phytoplankton. *Nature Climate Change*, 6(3), 323–330. <https://doi.org/10.1038/nclimate2838>

Cai, P., Zhao, D., Wang, L., Huang, B., & Dai, M. (2015). Role of particle stock and phytoplankton community structure in regulating particulate organic carbon export in a large marginal sea. *Journal of Geophysical Research: Oceans*, 120, 2063–2095. <https://doi.org/10.1002/2014JC010432>

Calbet, A., & Landry, M. R. (2004). Phytoplankton growth, microzooplankton grazing, and carbon cycling in marine systems. *Limnology and Oceanography*, 49(1), 51–57. <https://doi.org/10.4319/lo.2004.49.1.0051>

Calvo-Díaz, A., Morán, X. A. G., & Suárez, L. Á. (2008). Seasonality of picophytoplankton chlorophyll a and biomass in the central Cantabrian Sea, southern Bay of Biscay. *Journal of Marine Systems*, 72(1–4), 271–281. <https://doi.org/10.1016/j.jmarsys.2007.03.008>

Chang, J., Shiah, F., Gong, G., & Chiang, K. (2003). Cross-shelf variation in carbon-to-chlorophyll a ratios in the East China Sea, summer 1998. *Deep-Sea Research Part II: Topical Studies in Oceanography*, 50(6–7), 1237–1247. [https://doi.org/10.1016/S0967-0645\(03\)00020-1](https://doi.org/10.1016/S0967-0645(03)00020-1)

Chen, B. Z., Landry, M. R., Huang, B. Q., & Liu, H. B. (2012). Does warming enhance the effect of microzooplankton grazing on marine phytoplankton in the ocean? *Limnology and Oceanography*, 57(2), 519–526. <https://doi.org/10.4319/lo.2012.57.2.0519>

Chen, B. Z., Wang, L., Song, S. Q., Huang, B. Q., Sun, J., & Liu, H. B. (2011). Comparisons of picophytoplankton abundance, size, and fluorescence between summer and winter in northern South China Sea. *Continental Shelf Research*, 31(14), 1527–1540. <https://doi.org/10.1016/j.csr.2011.06.018>

Chen, Y. L. L., & Chen, H. Y. (2003). Nitrate-based new production and its relationship to primary production and chemical hydrography in spring and fall in the East China Sea. *Deep-Sea Research Part II-topical Studies in Oceanography*, 50(6–7), 1249–1264. [https://doi.org/10.1016/S0967-0645\(03\)00021-3](https://doi.org/10.1016/S0967-0645(03)00021-3)

Chen, Y. L. L., Chen, H. Y., Gong, G. C., Lin, Y. H., Jan, S., & Takahashi, M. (2004). Phytoplankton production during a summer coastal upwelling in the East China Sea. *Continental Shelf Research*, 24(12), 1321–1338. <https://doi.org/10.1016/j.csr.2004.04.002>

Chen, Y. L. L., Chen, H. Y., Lee, W. H., Hung, C. C., Wong, G. T. F., & Kanda, J. (2001). New production in the East China Sea, comparison between well-mixed winter and stratified summer conditions. *Continental Shelf Research*, 21(6–7), 751–764. [https://doi.org/10.1016/S0278-4343\(00\)00108-4](https://doi.org/10.1016/S0278-4343(00)00108-4)

Chen, Y. L. L., Lu, H. B., Shiah, F. K., Gong, G. C., Liu, K. K., & Kanda, J. (1999). New production and F-ratio on the continental shelf of the East China Sea: Comparisons between nitrate inputs from the subsurface Kuroshio current and the Changjiang River. *Estuarine, Coastal and Shelf Science*, 48(1), 59–75. <https://doi.org/10.1006/ecss.1999.0404>

Cullen, J. J., & Eppley, R. W. (1981). Chlorophyll maximum layers of the Southern-California Bight and possible mechanisms of their formation and maintenance. *Oceanologica Acta*, 4(1), 23–32.

Dore, J. E., & Karl, D. M. (1996). Nitrification in the euphotic zone as a source for nitrite, nitrate, and nitrous oxide at Station ALOHA. *Limnology and Oceanography*, 41(8), 1619–1628. <https://doi.org/10.4319/lo.1996.41.8.1619>

Dortch, Q. (1990). The interaction between ammonium and nitrate uptake in phytoplankton. *Marine Ecology Progress Series*, 61(1–2), 183–201. <https://doi.org/10.3354/meps061183>

Dugdale, R. C., & Goering, J. J. (1967). Uptake of new and regenerated forms of nitrogen in primary productivity. *Limnology and Oceanography*, 12(2), 196–206. <https://doi.org/10.4319/lo.1967.12.2.0196>

Eppley, R. W. (1972). Temperature and phytoplankton growth in the sea. *Fishery Bulletin*, 70(4), 1063–1085.

Eppley, R. W., Harrison, W. G., Chisholm, S. W., & Stewart, E. (1977). Particulate organic matter in surface waters off Southern California and its relationship to phytoplankton. *Journal of Marine Research*, 35, 671–695.

Eppley, R. W., & Peterson, B. J. (1979). Particulate organic matter flux and planktonic new production in the deep ocean. *Nature*, 282(5740), 677–680. <https://doi.org/10.1038/282677a0>

Falkowski, P. G., & Owens, T. G. (1980). Light-shade adaptation: Two strategies in marine phytoplankton. *Plant Physiology*, 66(4), 592–595. <https://doi.org/10.1104/pp.66.4.592>

Field, C. B., Behrenfeld, M. J., Randerson, J. T., & Falkowski, P. (1998). Primary production of the biosphere: Integrating terrestrial and oceanic components. *Science*, 281(5374), 237–240. <https://doi.org/10.1126/science.281.5374.237>

Flynn, K. J., Fasham, M. J. R., & Hipkin, C. R. (1997). Modelling the interactions between ammonium and nitrate uptake in marine phytoplankton. *Philosophical Transactions of the Royal Society of London Series B-Biological Sciences*, 352(1361), 1625–1645. <https://doi.org/10.1098/rstb.1997.0145>

Geider, R. J., MacIntyre, H. L., & Kana, T. M. (1996). A dynamic model of photoadaptation in phytoplankton. *Limnology and Oceanography*, 41(1), 1–15. <https://doi.org/10.4319/lo.1996.41.1.0001>

Geider, R. J., MacIntyre, H. L., & Kana, T. M. (1997). Dynamic model of phytoplankton growth and acclimation: Responses of the balanced growth rate and the chlorophyll a:carbon ratio to light, nutrient-limitation and temperature. *Marine Ecology Progress Series*, 148(1–3), 187–200. <https://doi.org/10.3354/meps148187>

- Gong, G. C., Wen, Y. H., Wang, B. W., & Liu, G. J. (2003). Seasonal variation of chlorophyll *a* concentration, primary production and environmental conditions in the subtropical East China Sea. *Deep-Sea Research Part II: Topical Studies in Oceanography*, *50*(6-7), 1219–1236. [https://doi.org/10.1016/S0967-0645\(03\)00019-5](https://doi.org/10.1016/S0967-0645(03)00019-5)
- Guo, C., Liu, H., Zheng, L., Song, S., Chen, B., & Huang, B. (2014). Seasonal and spatial patterns of picophytoplankton growth, grazing and distribution in the East China Sea. *Biogeosciences*, *11*(7), 1847–1862. <https://doi.org/10.5194/bg-11-1847-2014>
- Guo, S. J., Feng, Y. Y., Wang, L., Dai, M. H., Liu, Z. L., Bai, Y., & Sun, J. (2014). Seasonal variation in the phytoplankton community of a continental-shelf sea: The East China Sea. *Marine Ecology Progress Series*, *516*, 103–126. <https://doi.org/10.3354/meps10952>
- Harrison, P. J., Thompson, P. A., & Calderwood, G. S. (1990). Effects of nutrients and light limitation on the biochemical composition of phytoplankton. *Journal of Applied Phycology*, *2*(1), 45–56. <https://doi.org/10.1007/BF02179768>
- Harrison, P. J., Zingone, A., Mickelson, M. J., Lehtinen, S., Ramaiah, N., Kraberg, A. C., et al. (2015). Cell volumes of marine phytoplankton from globally distributed coastal data sets. *Estuarine, Coastal and Shelf Science*, *162*, 130–142. <https://doi.org/10.1016/j.ecss.2015.05.026>
- Hunter, B. L., & Laws, E. A. (1981). Atp and chlorophyll-*a* as estimators of phytoplankton carbon biomass. *Limnology and Oceanography*, *26*(5), 944–956. <https://doi.org/10.4319/lo.1981.26.5.0944>
- Jakobsen, H. H., & Markager, S. (2016). Carbon-to-chlorophyll ratio for phytoplankton in temperate coastal waters: Seasonal patterns and relationship to nutrients. *Limnology and Oceanography*, *61*(5), 1853–1868. <https://doi.org/10.1002/lno.10338>
- Kanda, J., Itoh, T., Ishikawa, D., & Watanabe, Y. (2003). Environmental control of nitrate uptake in the East China Sea. *Deep-Sea Research Part II: Topical Studies in Oceanography*, *50*(2), 403–422. [https://doi.org/10.1016/S0967-0645\(02\)00464-2](https://doi.org/10.1016/S0967-0645(02)00464-2)
- Knap, A. H., Michaels, A., Close, A. R., Ducklow, H., & Dickson, A. G. (1996). Protocols for the Joint Global Ocean Flux study (JGOFS) core measurements. JGOFS, Reprint of the IOC Manuals and Guides No. 29, UNESCO 1994, 19.
- Landry, M. R. (1993). Predicting excretion rates of microzooplankton from carbon metabolism and elemental ratios. *Limnology and Oceanography*, *38*(2), 468–472.
- Latasa, M. (2007). Improving estimations of phytoplankton class abundances using CHEMTAX. *Marine Ecology Progress Series*, *329*, 13–21. <https://doi.org/10.3354/meps329013>
- Laws, E. A., & Bannister, T. T. (1980). Nutrient-limited and light-limited growth of *Thalassiosira fluviatilis* in continuous culture, with implications for phytoplankton growth in the ocean. *Limnology and Oceanography*, *25*(3), 457–473. <https://doi.org/10.4319/lo.1980.25.3.0457>
- Laws, E. A., Bidigare, R. R., & Karl, D. M. (2016). Enigmatic relationship between chlorophyll *a* concentrations and photosynthetic rates at Station ALOHA. *Heliyon*, *2*(9), e00156. <https://doi.org/10.1016/j.heliyon.2016.e00156>
- Laws, E. A., & Chalup, M. S. (1990). A microalgal growth model. *Limnology and Oceanography*, *35*(3), 597–608. <https://doi.org/10.4319/lo.1990.35.3.0597>
- Legendre, L., & Michaud, J. (1999). Chlorophyll *a* to estimate the particulate organic carbon available as food to large zooplankton in the euphotic zone of oceans. *Journal of Plankton Research*, *21*(11), 2067–2083. <https://doi.org/10.1093/plankt/21.11.2067>
- Li, Q. P., Franks, P. J. S., Landry, M. R., Goericke, R., & Taylor, A. G. (2010). Modeling phytoplankton growth rates and chlorophyll to carbon ratios in California coastal and pelagic ecosystems. *Journal of Geophysical Research*, *115*, G04003. <https://doi.org/10.1029/2009JG001111>
- Lipschultz, F. (2001). A time-series assessment of the nitrogen cycle at BATS. *Deep-Sea Research Part II: Topical Studies in Oceanography*, *48*(8-9), 1897–1924. [https://doi.org/10.1016/S0967-0645\(00\)00168-5](https://doi.org/10.1016/S0967-0645(00)00168-5)
- Liu, S. M., Hong, G. H., Zhang, J., Ye, X. W., & Jiang, X. L. (2009). Nutrient budgets for large Chinese estuaries. *Biogeosciences*, *6*(10), 2245–2263. <https://doi.org/10.5194/bg-6-2245-2009>
- Liu, X., Furuya, K., Shiozaki, T., Masuda, T., Kodama, T., Sato, M., et al. (2013). Variability in nitrogen sources for new production in the vicinity of the shelf edge of the East China Sea in summer. *Continental Shelf Research*, *61–62*, 23–30. <https://doi.org/10.1016/j.csr.2013.04.014>
- Liu, X., Xiao, W., Landry, M. R., Chiang, K.-P., Wang, L., & Huang, B. (2016). Responses of phytoplankton communities to environmental variability in the East China Sea. *Ecosystems*, *19*(5), 832–849. <https://doi.org/10.1007/s10021-016-9970-5>
- Lyngsgaard, M. M., Markager, S., Richardson, K., Møller, E. F., & Jakobsen, H. H. (2017). How well does chlorophyll explain the seasonal variation in phytoplankton activity? *Estuaries and Coasts*, *40*(5), 1263–1275. <https://doi.org/10.1007/s12237-017-0215-4>
- Mackey, M. D., Mackey, D. J., Higgins, H. W., & Wright, S. W. (1996). CHEMTAX - A program for estimating class abundances from chemical markers: Application to HPLC measurements of phytoplankton. *Marine Ecology Progress Series*, *144*(1-3), 265–283. <https://doi.org/10.3354/meps144265>
- Marañón, E., Behrenfeld, M. J., González, N., Mourinho, B., & Zubkov, M. V. (2003). High variability of primary production in oligotrophic waters of the Atlantic Ocean: Uncoupling from phytoplankton biomass and size structure. *Marine Ecology Progress Series*, *257*, 1–11. <https://doi.org/10.3354/meps257001>
- Morel, A., & Berthon, J. F. (1989). Surface pigments, algal biomass profiles, and potential production of the euphotic layer: Relationships reinvestigated in view of remote-sensing applications. *Limnology and Oceanography*, *34*(8), 1545–1562. <https://doi.org/10.4319/lo.1989.34.8.1545>
- Olson, R. J., Zettler, E. R., & DuRand, M. D. (1993). Phytoplankton analysis using flow cytometry. In P. F. Kemp, B. F. Sherr, E. B. Sherr, & J. J. Cole (Eds.), *Handbook of methods in aquatic microbial ecology* (pp. 175–186). Boca Raton, FL: Lewis Publisher. <https://doi.org/10.1201/9780203752746>
- Platt, T., & Sathyendranath, S. (1988). Oceanic primary production: Estimation by remote sensing at local and regional scales. *Science*, *241*(4873), 1613–1620. <https://doi.org/10.1126/science.241.4873.1613>
- R Core Team (2016). *R: A language and environment for statistical computing*. Vienna, Austria: R Foundation for Statistical Computing. Open access available at: <http://cran.r-project.org>
- Sathyendranath, S., Stuart, V., Nair, A., Oka, K., Nakane, T., Bouman, H., et al. (2009). Carbon-to-chlorophyll ratio and growth rate of phytoplankton in the sea. *Marine Ecology Progress Series*, *383*, 73–84. <https://doi.org/10.3354/meps07998>
- Shuter, B. (1979). A model of physiological adaptation in unicellular algae. *Journal of Theoretical Biology*, *78*(4), 519–552. [https://doi.org/10.1016/0022-5193\(79\)90189-9](https://doi.org/10.1016/0022-5193(79)90189-9)
- Stemann Nielsen, E. (1952). The use of radio-active carbon (C^{14}) for measuring organic production in the sea. *Journal du Conseil*, *18*(2), 117–140. <https://doi.org/10.1093/icesjms/18.2.117>
- Strickland, J. D. H. (1960). *Measuring the production of marine phytoplankton*. Ottawa: Pacific Oceanographic Group, Nanaimo, B.C., Fisheries Research Board of Canada.
- Terry, K. L., Hirata, J., & Laws, E. A. (1983). Light-limited growth of two strains of the marine diatom *Phaeodactylum tricoratum* Bohlin: Chemical composition, carbon partitioning and the diel periodicity of physiological processes. *Journal of Experimental Marine Biology and Ecology*, *68*(3), 209–227. [https://doi.org/10.1016/0022-0981\(83\)90054-0](https://doi.org/10.1016/0022-0981(83)90054-0)

- Thompson, P. A., Harrison, P. J., & Parslow, J. S. (2004). Influence of irradiance on cell volume and carbon quota for ten species of marine phytoplankton. *Journal of Phycology*, *27*(3), 351–360. <https://doi.org/10.1111/j.0022-3646.1991.00351>
- Uitz, J., Claustre, H., Morel, A., & Hooker, S. B. (2006). Vertical distribution of phytoplankton communities in open ocean: An assessment based on surface chlorophyll. *Journal of Geophysical Research*, *111*, C08005. <https://doi.org/10.1029/2005JC003207>
- Utermöhl, H. (1958). Methods of collecting plankton for various purposes are discussed. *SIL Communications. 1953-1996*, 1–38. <https://doi.org/10.1080/05384680.1958.11904091>
- Xie, Y., Tilstone, G. H., Widdicombe, C., Woodward, E. M. S., Harris, C., & Barnes, M. K. (2015). Effect of increases in temperature and nutrients on phytoplankton community structure and photosynthesis in the western English Channel. *Marine Ecology Progress Series*, *519*, 61–73. <https://doi.org/10.3354/meps11101>
- Yamaguchi, H., Ishizaka, J., Siswanto, E., Son, Y. B., Yoo, S., & Kiyomoto, Y. (2013). Seasonal and spring interannual variations in satellite-observed chlorophyll-*a* in the Yellow and East China Seas: New datasets with reduced interference from high concentration of resuspended sediment. *Continental Shelf Research*, *59*, 1–9. <https://doi.org/10.1016/j.csr.2013.03.009>
- Yool, A., Martin, A. P., Fernandez, C., & Clark, D. R. (2007). The significance of nitrification for oceanic new production. *Nature*, *447*(7147), 999–1002. <https://doi.org/10.1038/nature05885>
- Zapata, M., Rodriguez, F., & Garrido, J. L. (2000). Separation of chlorophylls and carotenoids from marine phytoplankton: A new HPLC method using a reversed phase C₈ column and pyridine-containing mobile phases. *Marine Ecology Progress Series*, *195*, 29–45. <https://doi.org/10.3354/meps195029>
- Zhang, J. (1996). Nutrient elements in large Chinese estuaries. *Continental Shelf Research*, *16*(8), 1023–1045. [https://doi.org/10.1016/0278-4343\(95\)00055-0](https://doi.org/10.1016/0278-4343(95)00055-0)
- Zheng, L. P., Chen, B. Z., Liu, X., Huang, B. Q., Liu, H. B., & Song, S. Q. (2015). Seasonal variations in the effect of microzooplankton grazing on phytoplankton in the East China Sea. *Continental Shelf Research*, *111*, 304–315. <https://doi.org/10.1016/j.csr.2015.08.010>